THE JOURNAL OF PHYSICAL CHEMISTRY Letters

Letter

Cite This: J. Phys. Chem. Lett. 2018, 9, 1260−1264

pubs.acs.org/JPCL

Ion Channel Sensing: Are Fluctuations the Crux of the Matter?

Marina A. Kasimova,[†] Aysenur Yazici,[‡] Yevgen Yudin,[‡] Daniele Granata,[†] Michael L. Klein,[†] Tibor Rohacs,[‡] and Vincenzo Carnevale*[,†]

[†]Institute for Computational Molecular Science, Temple University, Philadelphia, Pennsylvania 19122, United States

[‡]Department of Pharmacology, Physiology and Neuroscience, Rutgers−New Jersey Medical School, Newark, New Jersey 07103, United States

Supporting Information

ABSTRACT: The nonselective cation channel TRPV1 is responsible for transducing noxious stimuli into action potentials propagating through peripheral nerves. It is activated by temperatures greater than 43 °C, while remaining completely nonconductive at temperatures lower than this threshold. The origin of this sharp response, which makes TRPV1 a biological temperature sensor, is not understood. Here we used molecular dynamics simulations and free energy calculations to characterize the molecular determinants of the transition between nonconductive and conductive states. We found that hydration of the pore and thus ion permeation depends critically on the polar character of its molecular surface: in this narrow hydrophobic enclosure, the motion of a polar side-chain is sufficient to stabilize either the dry or wet state. The conformation of this side-chain is in turn coupled to the hydration state of four peripheral cavities, which undergo a dewetting transition at the activation temperature.

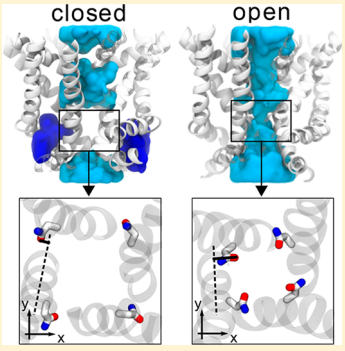

TRPV1 is an ion channel mostly expressed in the peripheral nervous system.[1,2] Upon activation, it generates the signal that, transmitted to the thalamus through the dorsal root ganglia, is perceived as a painful sensation.[3] This makes it an attractive pharmacological target to silence pain pathways.[4,5] However,the TRPV1 mechanism of activation and, in particular, its ability to sense temperature remains largely unexplained.[6−15]

Recent cryo-EM studies have revealed that TRPV1 is a tetrameric assembly with a transmembrane (TM) domain closely resembling that of voltage-gated ion channels:[16−18] it is composed of two main moduli: the S1−S4 domain and the pore domain connected through the S4−S5 linker. The pore domain contains the pathway for ions and is composed of the S5 and S6 helices from all four subunits.

Structures of TRPV1 resolved in different conformational states provided significant insight into its gating transitions.[16−18] It was shown that TRPV1 has two gates, upper and lower, located at the level of the selectivity filter (G643-M644) and of the S6 bundle crossing (I679), respectively. Both gates can be open (resiniferatoxin-bound or RTX-bound state) or closed (apo state); a particularly intriguing case is that of the capsaicin-bound (CAP-bound) state, in which the upper gate is closed, while the lower gate is partially dilated. Another interesting aspect of the CAP-bound state concerns its functional properties: it has been shown that the CAP-bound state is closed at low temperature, it has a 50% probability of opening at room temperature and it is completely open at high temperature.[19] While the microscopic determinants of this progressive activation are key to understand temperature sensing, it is still unclear how the channel transitions from the CAP-bound state to a conductive one.

We thus started by examining the differences between the three TRPV1 cryo-EM structures (apo, RTX-bound and CAP-bound). We aligned the S1−S4 domains, which do not undergo significant conformational rearrangements during gating, and compared the superimposed pore domains. Surprisingly, even though the CAP-bound state is putatively an intermediate state, we found it to be distinct from the other two, i.e., it differs from the apo and RTX-bound states more than the latter two differ from each other. Unlike the apo and RTX-bound conformations, in the CAP-bound one the S6 C-terminus moves away from the S4−S5 linker, indicating that these two elements are not physically in contact as they usually are in ion channels of the 6TM family (Figure 1a). This observation implies that TRPV1 opening occurs in two steps: uncoupling and recoupling of the S6 C-terminus and the S4−S5 linker. Based on the experimental data,[19] we speculate that the first step occurs already at low temperatures and hence it should be temperature-independent, while the second one is modulated by heat.

Partial detaching of the S6 C-terminus from the S4−S5 linker can result in the formation of small cavities between these two elements. Indeed, using a well-established method to detect voids and pockets in proteins (f-pocket[20]), in the CAP-bound state we found four cavities (one per channel subunit) hereafter referred to as peripheral cavities or PCs. These cavities are connected to the intracellular solution and run parallel to the central pore up to the middle of S6 (Figure 1b). Notably, in the

Received: December 23, 2017
Accepted: February 13, 2018
Published: February 13, 2018

DOI: 10.1021/acs.jpclett.7b03396
J. Phys. Chem. Lett. 2018, 9, 1260−1264

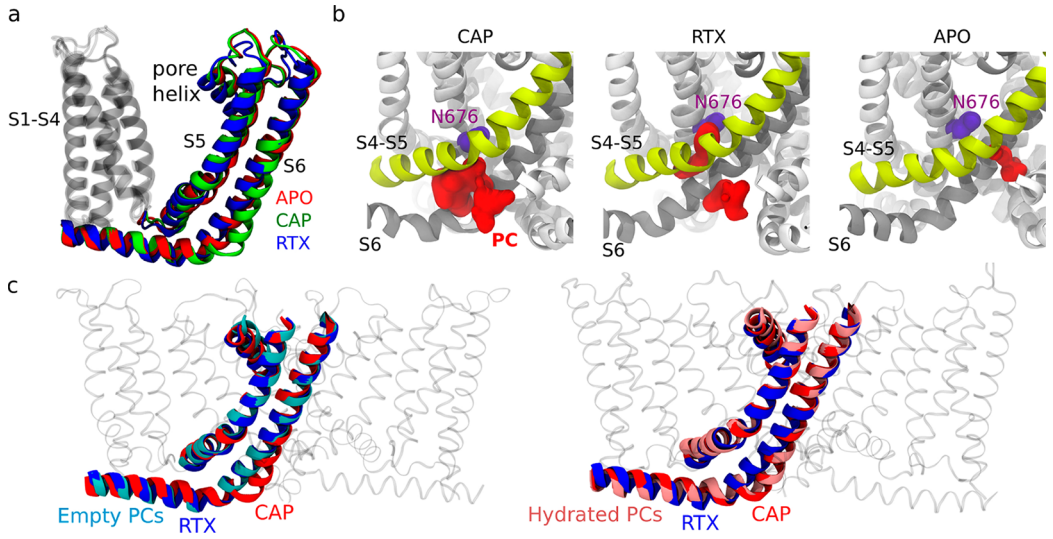

Figure 1. Comparison of the three cryo-EM structures, apo,[16] capsaicin-bound (CAP-bound)[17] and resiniferatoxin-bound (RTX-bound),[17] and the resulting conformations after the MD simulations. (a) Structural alignment of the three structures. (b) Analysis of the peripheral cavities (PCs, shown as red densities) in the three structures. (c) Representative subunits of the two MD trajectories: the channel with empty PCs on the left (the subunit in cyan almost coincides with the RTX-bound structure shown in blue) and the channel with hydrated PCs on the right (the subunit in pink almost coincides with the CAP-bound structure shown in red).

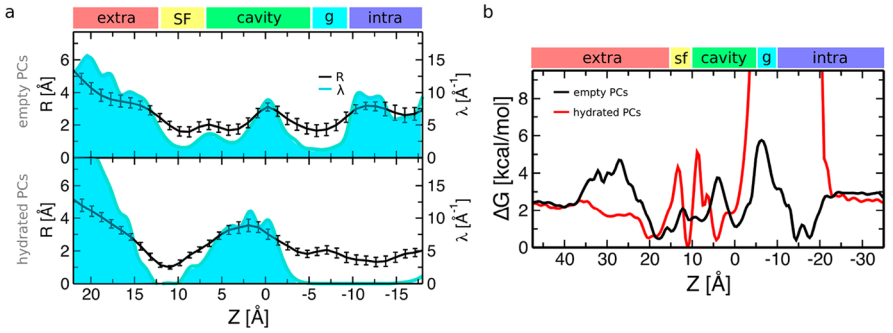

Figure 2. Analysis of the central pore in the channels with empty and hydrated PCs. (a) The plots show the average radius (black curve) and water density (cyan curve) profiles calculated for the second halves of the MD trajectories; top and bottom panels refer to empty and hydrated PCs, respectively. Error bars show the standard deviation. (b) Free energy profiles for permeation of a sodium ion in the conformations with empty (black) and hydrated (red) PCs. Note that in the first case, in addition to the free energy barrier at the level of the lower gate, there is one at the level of the central cavity (~3.2 kcal/mol). It is created by four Y671 residues, which are oriented perpendicular to the pore and create a constriction.[22] In the channel with hydrated PCs, however, Y671 adopts another conformation: these residues "open up" and become oriented parallel to the pore axis.[22] As a result, free energy barrier at the level of the central cavity disappears. Extra, SF, cavity, g, and intra denote the extracellular solution, selectivity filter, central cavity, lower gate and intracellular solution, respectively.

apo and RTX-bound states, homologous cavities are significantly smaller and not connected to the intracellular solution.

The presence of four PCs, accessible to the intracellular solution, made us hypothesize that these can host water molecules. Therefore, in modeling the initial configuration for molecular dynamics (MD) simulations, we filled these cavities with several water molecules (from 4 to 6) and considered a system with empty PCs as a control case. For each of them, a trajectory of 0.75 μs was generated (see SI Methods). Note that during these runs the PCs remained either hydrated if they were initially filled with water or dehydrated if they were initialized empty, suggesting that the channel admits two metastable states.

We thus analyzed the conformational rearrangements of the pore domain along the MD trajectories using, as reference, the three cryo-EM structures (apo, RTX-bound and CAP-bound). Figures S1 and 1c shows that the channel with hydrated PCs fluctuates in the region surrounding its initial structure, i.e., the CAP-bound state. Interestingly, the system in which the PCs remain empty drifts away from the CAP-bound state, and in particular, two out of four subunits converge to the RTX-bound state.

Encouraged by these observations, we asked whether the final configurations reached by the simulations with empty and hydrated PCs were, in fact, conductive and nonconductive states, respectively. Thus, we characterized the average radius and hydration profiles of the central pore for the two MD runs (Figure 2a and S2). We found that the profiles of the pore radius were qualitatively similar: the pore radius at the selectivity filter was ~1.5 and 1.1 Å for the channels with empty and hydrated PCs, respectively; that at the lower gate was 1.7 and 1.4 Å. By contrast, the two hydration profiles were drastically different: in the channel with hydrated PCs, we observed two hydrophobic gaps at the upper and lower gates, indicating that this state is nonconductive; however, in the other case, the central pore was completely hydrated,

DOI: 10.1021/acs.jpclett.7b03396
J. Phys. Chem. Lett. 2018, 9, 1260−1264

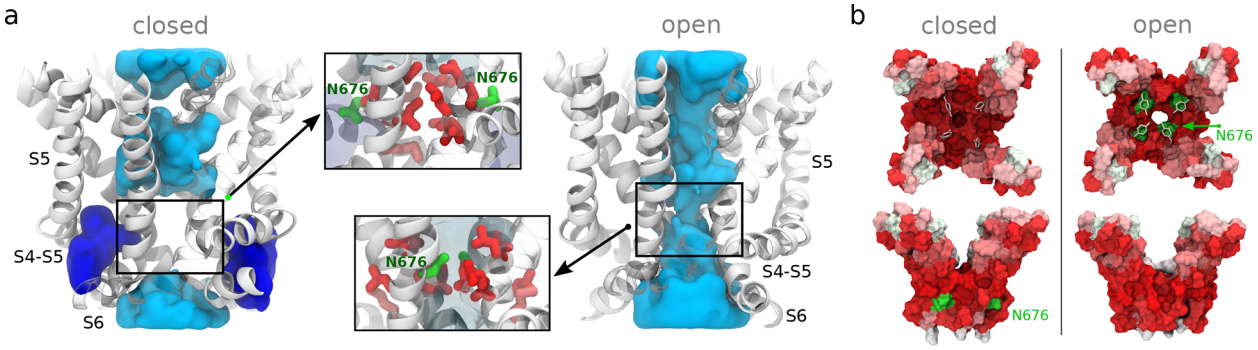

Figure 3. Polar character of the pore molecular surface. (a) Two different states of the TRPV1 channel, with hydrated (left) and empty (right) PCs. The average water density in the PCs and in the central pore is shown in blue and cyan, respectively. The two conformations of N676 (green) are shown in the insets. (b) Polar properties of the inner and outer surfaces of the S6 bundle in the closed (left) and open (right) states: top (top panel) and side (bottom panel) views. The residues in panels a and b are colored according to their polarity[26] (red−hydrophobic, and green−hydrophilic).

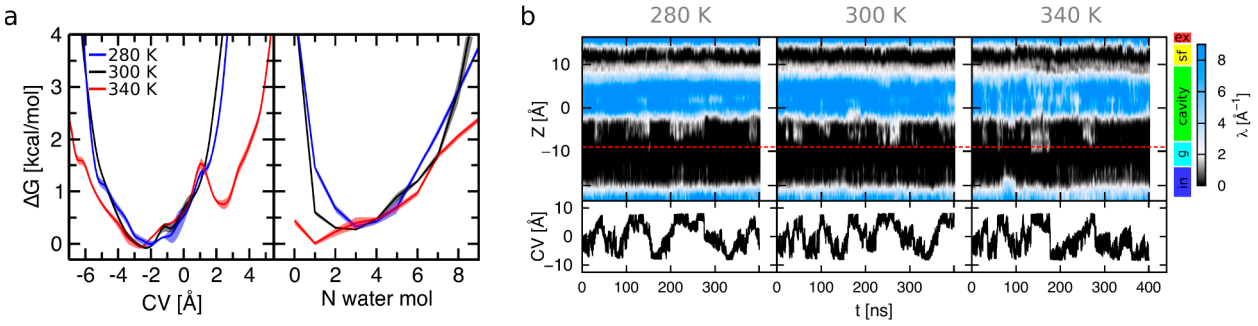

Figure 4. Temperature dependence of the N676 reorientation, hydration of the PC and the central pore. (a) Free energy profiles as a function of the N676 orientation (left) and the number of water molecules inside the PC (right). The blue line corresponds to the free energy profile at 280 K, black at 300 K and red at 340 K. The standard errors are shown as a shaded area around each profile. (b) Water density in the central pore at 280 K (top left), 300 K (top center) and 340 K (top right). The red dashed line separates the central cavity from the lower gate. Ex, sf, cavity, gate, and in correspond to the extracellular solution, selectivity filter, central cavity, lower gate and intracellular solution, respectively. The dynamics of the N676 orientation with respect to the central pore (bottom) is shown for comparison.

suggesting that the two gates are open. Importantly, in both the hydrated and the nonhydrated conformations, the pore size was smaller than the critical radius required to continuously hydrate hydrophobic cylindrical pores.[21]

Finally, for the two channel conformations, we estimated the free energy profile for permeation of a sodium ion using metadynamics[23] (Figure 2b; see also Figure S3a and S3b for the analysis of convergence). In the channel with hydrated PCs, we found a large free energy barrier, greater than 12 kcal/mol, at the level of the lower gate, confirming our hypothesis that this state is nonconductive. In the other conformation, however, the corresponding barrier was more than twice smaller (5.2 kcal/mol in the direction from extra- to intracellular solution), suggesting that emptying the PCs resulted in a conductive state.

Based on our analysis, we conclude that while the hydration of the PCs stabilized the closed state of the channel, their dehydration resulted in partial opening: two channel subunits have converged to the RTX-bound state, and the free energy barrier for a sodium ion permeation is only ∼2 kcal/mol larger than that in the fully open state.[24,25] For the sake of clarity, hereafter we will refer to the nonconductive and conductive conformations as closed and open, respectively.

What is then the major structural difference between the closed and open states? We noticed that one important difference is the conformation of a polar N676 (Figure 3a). When the channel is closed, N676 is exposed to the PCs, where it forms multiple hydrogen bonds with the resident water molecules, while the region of the central pore proximal to it is dehydrated. In the open state, instead, N676 faces the central pore, which is hydrated throughout its length and the PCs are devoid of waters; in the absence of N676, the residues lining the PCs are mostly hydrophobic (Figure S4a and S4b), and, rather than containing water, these cavities accommodate the side chains of M682, an amino acid that is located just two helix turns away from N676.

Another significant difference is the solvent accessible surface area (SASA) of residues lining the central pore (Figure S5 and 3b): for several hydrophobic residues (L674, L675, L678, and also Y671) this area is smaller in the open state, while for N676 it is larger, indicating that, the open pore is more hydrophilic than the closed one. Considering the similarity of the pore radius profiles in the closed and open states (Figure 2a), this result suggests that rather than the shape, what changes in the pore upon activation is the polar character of its surface.

The intriguing aspect of this observation is that the solvation free energy of hydrophobic moieties is known to show a nontrivial dependence on temperature. Is the transition from closed to open pore also temperature dependent? To test this hypothesis, we estimated the free energy profile of the N676 reorientation at room (300 K), high (340 K) and, as a control, low (280 K) temperature using metadynamics[23] (Figure 4a; see also Figures S6a,b and S7 for the definition of the collective variable and the analysis of convergence, respectively). Starting from the closed state, we performed 400 ns of metadynamics simulations at each temperature and sampled several transitions of N676 between the two conformations.

DOI: 10.1021/acs.jpclett.7b03396
J. Phys. Chem. Lett. 2018, 9, 1260−1264

In all three free energy profiles (Figure 4a), the state in which N676 is located inside the PC corresponds to the global minimum. However, at 340 K another free energy minimum appears corresponding to N676 facing the central pore. The difference between the two states does not exceed 1 kcal/mol and the barrier separating them is only 1.5 kcal/mol, suggesting that the two channel conformations are both significantly populated and in fast exchange. Importantly, the free energy profiles along an order parameter reporting the hydration of the adjacent PC shows that at 340 K the channel states with a hydrated and dehydrated PC coexist, while at 300 and 280 K the hydrated state is predominant. In summary, at 300 and 280 K the PC is filled with water, whereas at 340 K the PC experiences large amplitude water density fluctuations.

We also monitored the hydration of the central pore along the metadynamics runs, as this degree of freedom has a clear connection with ion conductance (Figure 4b). We found that in all three simulations, water molecules can transiently occupy the central cavity. However, only at 340 K, they can penetrate as deep as the lower gate. The hydration of this compartment was significantly increased at high temperature compared to room and low, even though in a fluctuating transient fashion.

At 340 K, the rotation of N676 is correlated with the hydration of the PC: if the PC is empty, then N676 points toward the pore; conversely, if the PC is hydrated, then N676 points outward, facing the PC (Figure S8). Moreover, the hydration of the pore is strongly correlated with the rotation of N676; as a result, the pore is empty if N676 points outward, while it becomes hydrated whenever N676 rotates toward the pore (Figure S9). Overall, the hydration of the PC, the rotation of N676, and the hydration of the pore are all strongly coupled with each other.

Do these wetting/dewetting phenomena play any role in the temperature dependence observed in our simulations? Simple thermodynamics arguments suggest a possible connection between the equilibrium properties of the waters confined in the PCs and the stability of the conductive conformation (see SI for a formal derivation). In particular, if the heat capacity of the open state is larger than that of the closed one, an increase in temperature can trigger the opening of the channel. We hypothesize that the dewetting of the PCs (the microscopic-length-scale analogue of a liquid−vapor transition) might be responsible for this increase in heat capacity. Indeed, the probability distribution function of PCs hydration number is approximately Gaussian at 280 and 300 K (Figure 4a). By contrast, at 340 K, the free energy profile "flattens out" and the PC can host, with approximately equal probability, zero, one, or more water molecules (Figure 4a). This "critical" behavior ought to be responsible for a sudden increase in heat capacity. Water confined in small hydrophobic cavities (of size comparable to the PCs) show peaks in the plot of C_p vs T as large as 20 kcal/mol/K upon melting.[27−29] Under the conditions considered in this work, this value can produce a stabilization of the open state of approximately −3.5 kcal/mol (see SI for details), a value in remarkable agreement with the $\Delta\Delta G$ extrapolated from our free energy profiles. We note, however, that the mechanism of TRPV1 temperature activation is more complex and possibly involves several channel regions.[6−15,30] Importantly, while the turret deletion channel used in our study does retain temperature sensitivity, the conclusions based on this construct should be regarded as tentative if transferred to the wild type TRPV1.

In summary, we find that the closed to open transition in a temperature-sensitive channel is triggered by small perturbations, which are, nonetheless, sufficient to alter the hydration of the channel pore: the rotation of N676 alters the hydrophobic character of the molecular surface lining the pore, thereby affecting its hydration and ion permeation. Susceptibility to perturbations is not uncommon in the pores of ion channels. Liquid−vapor oscillations have been reported several times[31−42] and are, arguably, the result of a precise evolutionary optimization: due to a fine-tuned hydrophobicity, pores undergoing hydrophobic gating are poised to transition and therefore maximally responsive to activating stimuli. In the case of TRPV1, the structural element exhibiting liquid−vapor oscillations is a pocket on the surface of the cytosolic side of the channel: interestingly, concave nonpolar surfaces have been shown to enhance water density fluctuations.[43] Finally, since the dehydration of small hydrophobic cavities shows strong dependence also on pressure and osmolarity, our simulations raise the intriguing hypothesis that a unified activation mechanism might underlie activation of TRPV channels by diverse external stimuli, such as osmotic stress[44] and hydrostatic pressure.[45]

■ ASSOCIATED CONTENT

Supporting Information

The Supporting Information is available free of charge on the ACS Publications website at DOI: 10.1021/acs.jpclett.7b03396.

Experimental methods and supplementary figures (PDF)

■ AUTHOR INFORMATION

Corresponding Author

*E-mail: vincenzo.carnevale@temple.edu.

ORCID

Vincenzo Carnevale: 0000-0002-1918-8280

Notes

The authors declare no competing financial interest.

■ ACKNOWLEDGMENTS

This work was supported in part by the National Institute of General Medical Sciences of the National Institutes of Health under award numbers R01GM093290, S10OD020095 and P01GM055876. We also acknowledge support from the National Science Foundation under award numbers ACI-1614804 and CNS-1625061.

■ REFERENCES

(1) Caterina, M. J.; Schumacher, M. A.; Tominaga, M.; Rosen, T. A.; Levine, J. D.; Julius, D. The Capsaicin Receptor: A Heat-Activated Ion Channel in the Pain Pathway. *Nature* **1997**, *389* (6653), 816−824.

(2) Hayes, P.; Meadows, H. J.; Gunthorpe, M. J.; Harries, M. H.; Duckworth, D. M.; Cairns, W.; Harrison, D. C.; Clarke, C. E.; Ellington, K.; Prinjha, R. K.; et al. Cloning and Functional Expression of a Human Orthologue of Rat Vanilloid Receptor-1. *Pain* **2000**, *88* (2), 205−215.

(3) Julius, D.; Basbaum, A. I. Molecular Mechanisms of Nociception. *Nature* **2001**, *413* (6852), 203−210.

(4) Szallasi, A.; Cortright, D. N.; Blum, C. A.; Eid, S. R. The Vanilloid Receptor TRPV1:10 Years from Channel Cloning to Antagonist Proof-of-Concept. *Nat. Rev. Drug Discovery* **2007**, *6* (5), 357−372.

(5) Carnevale, V.; Rohacs, T. TRPV1: A Target for Rational Drug Design. *Pharmaceuticals* **2016**, *9* (3), 52.

DOI: 10.1021/acs.jpclett.7b03396
J. Phys. Chem. Lett. 2018, 9, 1260−1264

(6) Yao, J.; Liu, B.; Qin, F. Modular Thermal Sensors in Temperature-Gated Transient Receptor Potential (TRP) Channels. *Proc. Natl. Acad. Sci. U. S. A.* **2011**, *108* (27), 11109−11114.
(7) Brauchi, S.; Orta, G.; Salazar, M.; Rosenmann, E.; Latorre, R. A Hot-Sensing Cold Receptor: C-Terminal Domain Determines Thermosensation in Transient Receptor Potential Channels. *J. Neurosci.* **2006**, *26* (18), 4835−4840.
(8) Grandl, J.; Kim, S. E.; Uzzell, V.; Bursulaya, B.; Petrus, M.; Bandell, M.; Patapoutian, A. Temperature-Induced Opening of TRPV1 Ion Channel Is Stabilized by the Pore Domain. *Nat. Neurosci.* **2010**, *13* (6), 708−714.
(9) Cordero-Morales, J. F.; Gracheva, E. O.; Julius, D. Cytoplasmic Ankyrin Repeats of Transient Receptor Potential A1 (TRPA1) Dictate Sensitivity to Thermal and Chemical Stimuli. *Proc. Natl. Acad. Sci. U. S. A.* **2011**, *108* (46), E1184−E1191.
(10) Zheng, W.; Qin, F. A Combined Coarse-Grained and All-Atom Simulation of TRPV1 Channel Gating and Heat Activation. *J. Gen. Physiol.* **2015**, *145* (5), 443−456.
(11) Brauchi, S.; Orta, G.; Mascayano, C.; Salazar, M.; Raddatz, N.; Urbina, H.; Rosenmann, E.; Gonzalez-Nilo, F.; Latorre, R. Dissection of the Components for PIP2 Activation and Thermosensation in TRP Channels. *Proc. Natl. Acad. Sci. U. S. A.* **2007**, *104* (24), 10246−10251.
(12) Vlachová, V.; Teisinger, J.; Susánková, K.; Lyfenko, A.; Ettrich, R.; Vyklický, L. Functional Role of C-Terminal Cytoplasmic Tail of Rat Vanilloid Receptor 1. *J. Neurosci.* **2003**, *23* (4), 1340−1350.
(13) Kim, S. E.; Patapoutian, A.; Grandl, J. Single Residues in the Outer Pore of TRPV1 and TRPV3 Have Temperature-Dependent Conformations. *PLoS One* **2013**, *8* (3), e59593.
(14) Chugunov, A. O.; Volynsky, P. E.; Krylov, N. A.; Nolde, D. E.; Efremov, R. G. Temperature-Sensitive Gating of TRPV1 Channel as Probed by Atomistic Simulations of Its Trans- and Juxtamembrane Domains. *Sci. Rep.* **2016**, *6*, 33112.
(15) Valente, P.; García-Sanz, N.; Gomis, A.; Fernández-Carvajal, A.; Fernández-Ballester, G.; Viana, F.; Belmonte, C.; Ferrer-Montiel, A. Identification of Molecular Determinants of Channel Gating in the Transient Receptor Potential Box of Vanilloid Receptor I. *FASEB J.* **2008**, *22* (9), 3298−3309.
(16) Liao, M.; Cao, E.; Julius, D.; Cheng, Y. Structure of the TRPV1 Ion Channel Determined by Electron Cryo-Microscopy. *Nature* **2013**, *504* (7478), 107−112.
(17) Cao, E.; Liao, M.; Cheng, Y.; Julius, D. TRPV1 Structures in Distinct Conformations Reveal Activation Mechanisms. *Nature* **2013**, *504* (7478), 113−118.
(18) Gao, Y.; Cao, E.; Julius, D.; Cheng, Y. TRPV1 Structures in Nanodiscs Reveal Mechanisms of Ligand and Lipid Action. *Nature* **2016**, *534* (7607), 347−351.
(19) Jara-Oseguera, A.; Bae, C.; Swartz, K. J. An External Sodium Ion Binding Site Controls Allosteric Gating in TRPV1 Channels. *eLife* **2016**, *5*, e13356.
(20) Le Guilloux, V.; Schmidtke, P.; Tuffery, P. Fpocket: An Open Source Platform for Ligand Pocket Detection. *BMC Bioinf.* **2009**, *10*, 168.
(21) Beckstein, O.; Sansom, M. S. P. Liquid−vapor Oscillations of Water in Hydrophobic Nanopores. *Proc. Natl. Acad. Sci. U. S. A.* **2003**, *100* (12), 7063−7068.
(22) Steinberg, X.; Kasimova, M. A.; Cabezas-Bratesco, D.; Galpin, J. D.; Ladron-de-Guevara, E.; Villa, F.; Carnevale, V.; Islas, L.; Ahern, C. A.; Brauchi, S. E. Conformational Dynamics in TRPV1 Channels Reported by an Encoded Coumarin Amino Acid. *eLife* **2017**, *6*, e28626.
(23) Laio, A.; Parrinello, M. Escaping Free-Energy Minima. *Proc. Natl. Acad. Sci. U. S. A.* **2002**, *99* (20), 12562−12566.
(24) Darré, L.; Furini, S.; Domene, C. Permeation and Dynamics of an Open-Activated TRPV1 Channel. *J. Mol. Biol.* **2015**, *427* (2), 537−549.
(25) Jorgensen, C.; Furini, S.; Domene, C. Energetics of Ion Permeation in an Open-Activated TRPV1 Channel. *Biophys. J.* **2016**, *111* (6), 1214−1222.
(26) Hessa, T.; Kim, H.; Bihlmaier, K.; Lundin, C.; Boekel, J.; Andersson, H.; Nilsson, I.; White, S. H.; von Heijne, G. Recognition of Transmembrane Helices by the Endoplasmic Reticulum Translocon. *Nature* **2005**, *433* (7024), 377−381.
(27) Vaitheeswaran, S.; Yin, H.; Rasaiah, J. C.; Hummer, G. Water Clusters in Nonpolar Cavities. *Proc. Natl. Acad. Sci. U. S. A.* **2004**, *101* (49), 17002−17005.
(28) Wang, L.; Zhao, J.; Fang, H. Water Clusters Confined in Nonpolar Cavities by Ab Initio Calculations. *J. Phys. Chem. C* **2008**, *112* (31), 11779−11785.
(29) Nigra, P.; Carignano, M. A.; Kais, S. Study of Phase Changes of the Water Octamer Using Parallel Tempering and Multihistogram Methods. *J. Chem. Phys.* **2001**, *115* (6), 2621−2628.
(30) García-Sanz, N.; Valente, P.; Gomis, A.; Fernández-Carvajal, A.; Fernández-Ballester, G.; Viana, F.; Belmonte, C.; Ferrer-Montiel, A. A Role of the Transient Receptor Potential Domain of Vanilloid Receptor I in Channel Gating. *J. Neurosci.* **2007**, *27* (43), 11641−11650.
(31) Anishkin, A.; Sukharev, S. Water Dynamics and Dewetting Transitions in the Small Mechanosensitive Channel MscS. *Biophys. J.* **2004**, *86* (5), 2883−2895.
(32) Anishkin, A.; Akitake, B.; Kamaraju, K.; Chiang, C.-S.; Sukharev, S. Hydration Properties of Mechanosensitive Channel Pores Define the Energetics of Gating. *J. Phys.: Condens. Matter* **2010**, *22* (45), 454120.
(33) Sotomayor, M.; Schulten, K. Molecular Dynamics Study of Gating in the Mechanosensitive Channel of Small Conductance MscS. *Biophys. J.* **2004**, *87* (5), 3050−3065.
(34) Birkner, J. P.; Poolman, B.; Koçer, A. Hydrophobic Gating of Mechanosensitive Channel of Large Conductance Evidenced by Single-Subunit Resolution. *Proc. Natl. Acad. Sci. U. S. A.* **2012**, *109* (32), 12944−12949.
(35) Nury, H.; Poitevin, F.; Van Renterghem, C.; Changeux, J.-P.; Corringer, P.-J.; Delarue, M.; Baaden, M. One-Microsecond Molecular Dynamics Simulation of Channel Gating in a Nicotinic Receptor Homologue. *Proc. Natl. Acad. Sci. U. S. A.* **2010**, *107* (14), 6275−6280.
(36) Zhu, F.; Hummer, G. Pore Opening and Closing of a Pentameric Ligand-Gated Ion Channel. *Proc. Natl. Acad. Sci. U. S. A.* **2010**, *107*, 19814.
(37) Zhu, F.; Hummer, G. Drying Transition in the Hydrophobic Gate of the GLIC Channel Blocks Ion Conduction. *Biophys. J.* **2012**, *103* (2), 219−227.
(38) Aryal, P.; Abd-Wahab, F.; Bucci, G.; Sansom, M. S. P.; Tucker, S. J. A Hydrophobic Barrier Deep within the Inner Pore of the TWIK-1 K2P Potassium Channel. *Nat. Commun.* **2014**, *5*, 4377.
(39) Dong, H.; Fiorin, G.; Carnevale, V.; Treptow, W.; Klein, M. L. Pore Waters Regulate Ion Permeation in a Calcium Release-Activated Calcium Channel. *Proc. Natl. Acad. Sci. U. S. A.* **2013**, *110* (43), 17332−17337.
(40) Jensen, M. Ø.; Borhani, D. W.; Lindorff-Larsen, K.; Maragakis, P.; Jogini, V.; Eastwood, M. P.; Dror, R. O.; Shaw, D. E. Principles of Conduction and Hydrophobic Gating in K+ Channels. *Proc. Natl. Acad. Sci. U. S. A.* **2010**, *107* (13), 5833−5838.
(41) Aryal, P.; Sansom, M. S. P.; Tucker, S. J. Hydrophobic Gating in Ion Channels. *J. Mol. Biol.* **2015**, *427* (1), 121−130.
(42) Trick, J. L.; Aryal, P.; Tucker, S. J.; Sansom, M. S. P. Molecular Simulation Studies of Hydrophobic Gating in Nanopores and Ion Channels. *Biochem. Soc. Trans.* **2015**, *43* (2), 146−150.
(43) Xi, E.; Venkateshwaran, V.; Li, L.; Rego, N.; Patel, A. J.; Garde, S. Hydrophobicity of Proteins and Nanostructured Solutes Is Governed by Topographical and Chemical Context. *Proc. Natl. Acad. Sci. U. S. A.* **2017**, *114* (51), 13345−13350.
(44) Zaelzer, C.; Hua, P.; Prager-Khoutorsky, M.; Ciura, S.; Voisin, D. L.; Liedtke, W.; Bourque, C. W. ΔN-TRPV1: A Molecular Co-Detector of Body Temperature and Osmotic Stress. *Cell Rep.* **2015**, *13* (1), 23−30.
(45) Gao, J.; Sun, X.; White, T. W.; Delamere, N. A.; Mathias, R. T. Feedback Regulation of Intracellular Hydrostatic Pressure in Surface Cells of the Lens. *Biophys. J.* **2015**, *109* (9), 1830−1839.

DOI: 10.1021/acs.jpclett.7b03396
J. Phys. Chem. Lett. 2018, 9, 1260−1264